Boletim da Sociedade Astronômica Brasileira, **30**, no. 1, 239-240

The FLASK code: beyond lognormal models of cosmological fields

Henrique S. Xavier[1,2], Filipe B. Abdalla[1], & Benjamin Joachimi[1]

[1] University College London (UK)
[2] University of Sao Paulo (Brazil) e-mail: hsxavier@if.usp.br

Abstract. It is common in cosmology to model either the matter density or the weak lensing convergence as lognormal fields; however, jointly modelling them is impossible. We propose two ways of overcoming this limitation: distorting the fields' power spectra; or obtaining the convergence from a line-of-sight integration of the lognormal density. The latter results in an analytical prediction for the skewness of the convergence distribution. We present the code FLASK, which creates tomographic realisations on the sphere of an arbitrary number of correlated lognormal fields, and show that it works for clustering and lensing with sub-per-cent accuracy over relevant angular scales and redshift ranges.

Resumo. É comum na cosmologia modelar a densidade da matéria ou a convergência de lentes fracas como campos lognormais; porém, a modelagem conjunta desses dois campos é impossível. Nós propomos duas formas de superar essa limitação: distorcendo os espectros de potência dos campos ou integrando a densidade lognormal sobre a linha de visada. A última abordagem também resulta em uma previsão analítica para a obliquidade da distribuição de convergência. Apresentamos o código FLASK, que gera realizações tomográficas na esfera de um número arbitrário de campos lognormais correlacionados, e mostramos que ele pode criar simulações conjuntas de distribuição de galáxias e lentes com precisão de sub-percentagem nas escalas angulares e intervalos de *redshift* relevantes.

Keywords. methods: statistical – gravitational lensing: weak – large-scale structure of Universe

1. Lognormal limitations

A lognormal random variable X is derived from a standard (zero mean, unit variance) Gaussian variable Z through the formula:

$$X = e^{\mu+\sigma Z} - \lambda. \tag{1}$$

Lognormals are better models to the density and convergence distributions than Gaussians because: They have a hard lower limit ($X \geq -\lambda$); and they have long tails at high values.

If two Gaussian variables Z_1 and Z_2 that have covariance ξ_g are used to generate lognormal variables X_1 and X_2, the covariance of the lognormal variables will be:

$$\xi_{ln} = (\langle X_1\rangle + \lambda_1)(\langle X_2\rangle + \lambda_2)(e^{\xi_g} - 1), \tag{2}$$

where $\langle X_i\rangle$ is the mean of X_i. Therefore, the relation between the Pearson correlation coefficients ρ_g and ρ_{ln} of the Gaussian and lognormal variables is given by Fig. 1. We notice that the correlation between lognormal variables is limited to a interval smaller than $[-1, +1]$. This happens because the relation between two lognormal variables with different skewnesses is non-linear.

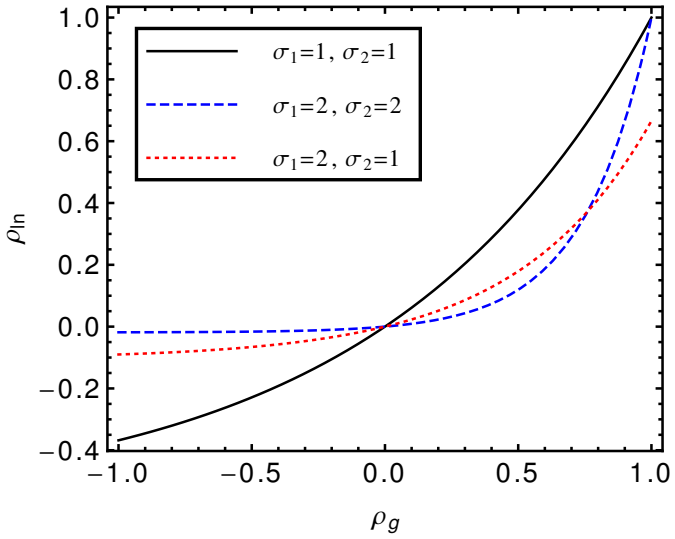

Figure 1. Relationship between the correlation ρ_g of two Gaussian variables and the correlation ρ_{ln} of their associated lognormal variables.

2. Consequences in cosmology

The limitations presented in Sec. 1 do not affect independent simulations of density nor of convergence. However, this is not the case for their joint simulations, in which the covariance matrices that describe the fields – given by their auto and cross power spectra – are unattainable by lognormal variables: as Fig. 2 shows, the amount of distortion that would have to be applied to the angular power spectra to make them lognormal compliant can be significantly large.

This happens because the relation between density and convergence enforces that both cannot be lognormals at the same time. The convergence κ at a line of sight (LoS) $\boldsymbol{\theta}$ for sources at redshift z_s is given by a weighted integral of the matter density contrast δ:

$$\kappa(\boldsymbol{\theta}, z_s) = \int_0^{z_s} K(z, z_s)\delta(\boldsymbol{\theta}, z)\mathrm{d}z. \tag{3}$$

While a sum of Gaussian variables is also a Gaussian variable, a sum (or integral) of lognormal variables is *not* a lognormal variable. Enforcing a power spectra derived from Eq. 3 at the same time one enforces all distributions to be lognormals is like enforcing two different angles for a triangle with equal sides. Therefore, one must either adopt different power spectra or different distributions.

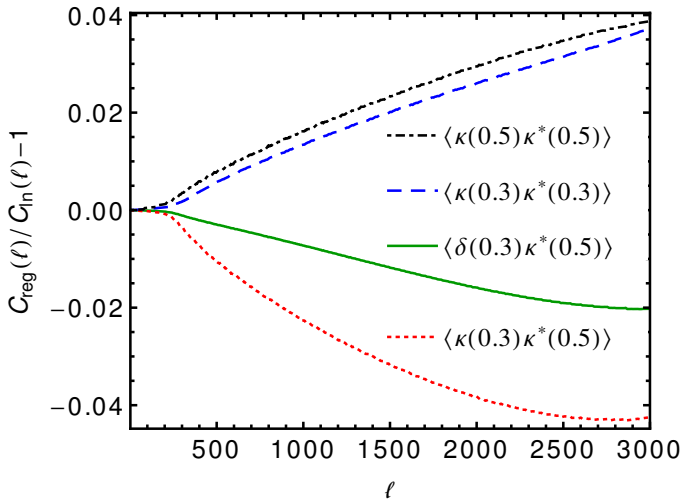

Figure 2. Fractional differences between the original angular power spectra $C^{ij}_{\rm ln}(\ell)$ and the regularised one $C^{ij}_{\rm reg}(\ell)$ when modelling density and convergence at three redshift bins.

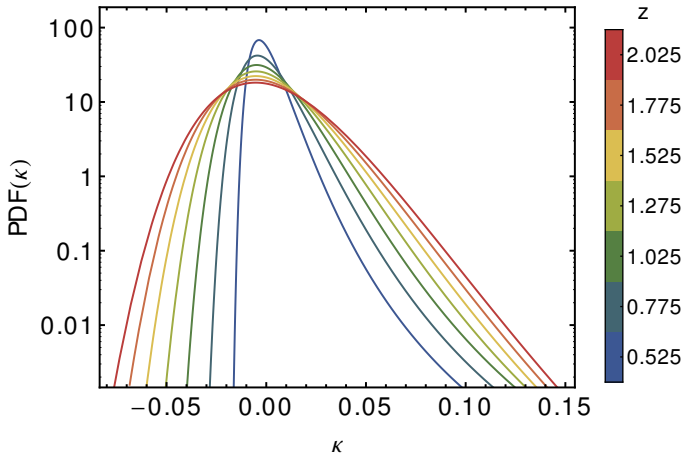

Figure 3. Distributions for the convergence obtained from lognormal density LoS integration, for various redshifts.

3. A different convergence PDF

Instead of assuming κ to be lognormal, one can compute it by LoS integration of the lognormal density field. The resulting distribution is shown as a function of redshift in Fig. 3.

The convergences obtained from density LoS integration should follow the theoretical $C^{ij}(\ell)$s exactly. Due to the approximation of the integral by a sum, however, they will slightly diverge in a predictable way. Fig. 4 shows that we can perfectly predict this deviation and that we can reproduce the true convergence power spectra up to one per cent on the relevant redshift ranges and angular scales.

Finally, this lognormal density LoS integration approach can be used to compute an analytic prediction for the skewness of the convergence distribution:

$$\mathrm{Skew}[\kappa(z_{\rm s})] = \frac{1}{\mathrm{Var}^{3/2}[\kappa(z_{\rm s})]} \iiint_0^{z_{\rm s}} K(z_1,z_{\rm s})K(z_2,z_{\rm s})K(z_3,z_{\rm s})\cdot$$
$$[3\xi_{\delta\delta}(z_1,z_2)\xi_{\delta\delta}(z_2,z_3) + \xi_{\delta\delta}(z_1,z_2)\xi_{\delta\delta}(z_2,z_3)\xi_{\delta\delta}(z_3,z_1)]\mathrm{d}z_1\mathrm{d}z_2\mathrm{d}z_3, \quad (4)$$

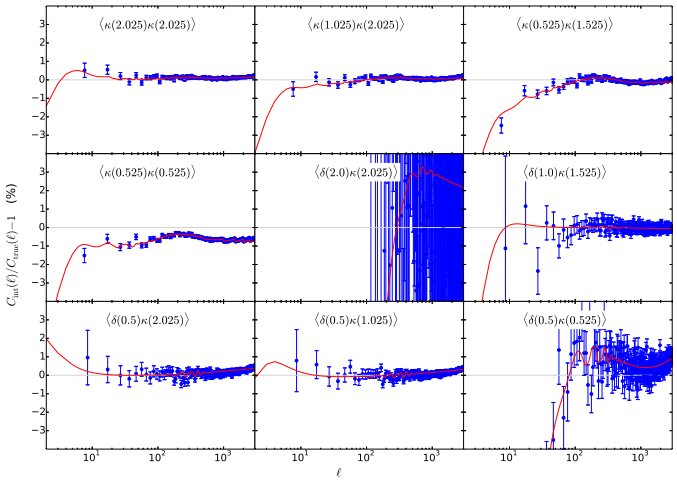

Figure 4. Fractional difference between the convergence $C(\ell)$ computed as a LoS Riemann sum of the simulated density, $C_{\rm int}(\ell)$, and the true one, $C_{\rm true}(\ell)$. The red curves show the theoretical expectation given the numerical approximations, and the blue data points show the average of 1000 independent simulations. The first four (last five) subplots show the results for convergence–convergence (density–convergence) power spectra. The density was simulated in 40 redshift bins of width $\Delta z = 0.05$.

where $\xi_{\delta\delta}(z,z') = \langle\delta(\boldsymbol{\theta},z)\delta(\boldsymbol{\theta},z')\rangle$ is the matter density contrast LoS correlation function.

4. The FLASK simulation code

The open-source, parallel simulation code FLASK[1] discretizes the universe around the observer into many redshift shells, each described by a HEALPIX map, and generates Gaussian or lognormal (or sum of lognormals) realisations of an arbitrary number of correlated fields on these shells (e.g. multiple galaxy populations, convergence, shear and CMB temperature maps). Effects such as magnification bias, redshift space distortions and intrinsic alignments can be included by providing to FLASK the appropriate input $C^{ij}(\ell)$s. Density tracers can be Poisson sampled and have ellipticities assigned to them. FLASK can output full-sky HEALPIX maps and catalogues.

Acknowledgements. HSX acknowledges FAPESP for the financial support.

References

Xavier H. S., Abdalla F. B., Joachimi, B. 2016, MNRAS 459, 3693

[1] `http://www.astro.iag.usp.br/~flask`